The pseudogaps in multiband electron-doped cuprate superconductivity

N. Kristoffel^{† 1}, P. Rubin[†]

[†]Institute of Physics, University of Tartu, Riia 142, 51014 Tartu, Estonia

Abstract

The pseudogap (PG) excitations in the framework of multiband superconductivity are analysed. Calculations for the doping phase diagram of electron-doped cuprate superconductors have been made. A nonrigid multiband model has been used. The interband pairing acts between the upper Hubbard band (UHB) and midgap states created (and shifted upwards) by doping. The appearance of two PG and two phase diagram critical points (CP) is suggested. The larger antinodal PG reflects the destruction of the long-range antiferromagnetic (AF) order. The second, smaller PG is a near-nodal event with exposed doping dependence behind the first CP. It reaches the T_c - dome. Model calculations have been made. The peculiarities of the phase diagram are determined by the doping-stimulated band overlap dynamics. The observation of ,,foreign" carriers as compared to the ones introduced by doping is expected to start with the vanishing PG.

PACS: 74.20.-z; 74.72.-h; 74.25.Dw

Key words: Electron-doped cuprates; Superconductivity; Pseudogaps

1 Introduction

The concept of the pseudogap has born from the analysis of hole-doped cuprate superconductor low-energy excitations. An extensive literature exists concerning this feature and its interpretation [1-9]. The PG has been identified by various experimental methods and seems to be a characteristic phenomenon of doped cuprate superconductors. It is nearly material-independent [10]. The PG is exposed also in the normal state material at $T>T_c$. This is in essential contrast with the true strongly material dependent superconducting gap (SCG) observed at $T<T_c$. There have been misunderstandings in literature in discussing various gaps

¹ Corresponding author: E-mail: kolja@fi.tartu.ee

in comparable conditions. The PG can enter the superconductivity dome and be observable in this region as a normal state gap (NSG) [11]. Below T_c the PG can remain masked by the excitations of superconducting states. At a fixed doping there is no transformation of the PG into a SCG.

The magnitude of the PG is usually characterized by a temperature T* which is strongly doping-dependent. This T* line does not represent a real phase transition [12, 13]. The PG cannot be directly jointed to the superconducting order through its fluctuations in the normal state. One has shown that these fluctuations are quenched far below T* [14-16].

At present the origin of the PG is attributed to extrinsic genesis in respect of superconductivity [2, 6, 14, 16-19]. The formation of the PG can be associated with various types of the orderings of lattice and electronic nature [20-25], accompanied also with time reversal, spatial rotations and translation symmetry breaking [26, 27].

These orderings can be competitive with superconductivity in distinct momentum regions which otherwise participate in pairing. Then a depletion of excitation density around the Fermi energy appears.

The presence of a magnetic counterpart of the charge-channel PG has also been reported [1, 16, 28]. In general, the role of the spin-subsystem remains in the PG aspect not well understood.

Both the PG and the SCG appear as quasiparticle-type excitations. However, the SCG is of coherent- and the PG of noncoherent nature excitation [26, 29, 30]. These gaps can represent the actions of different momentum space regions at the same dopings.

The cuprate superconductivity is initiated by a necessary doping process. The first major result of this procedure is the metallization of the sample. It means that the chemical potential (μ) must lie in a partially filled band of the doping influenced spectrum. The basic (AF) order of cuprate becomes destroyed. The distortions of the crystal interior, which create the PG in the spectrum of the doped material, appear. This process at very low dopings is better known for hole-doped samples. It starts by forming hole-centered ferrons [31] on AF networks [32, 33]. An extended doping stimulates the percolation of such mesoscopic dopants-associated CuO_2 plane plaquettes [32]. A recent paper [34] has followed on the atomic scale the evolution of the electron structure from an insulator to superconductor, passing some kind of weak insulator state. The PG becomes built up on the background of the weakening of AF correlations with an extended doping. For electron-doped systems, where the AF and superconducting domains overlap markedly, the problem needs further investigations.

The PG and the SCG can be observed in the same underdoped region. The energy scales for these two types of gaps are here rather different, as also their development with doping are opposite. The PG diminishes, the SCG grows with doping. This is the simplest indication to differentiate them. Coming nearer to the critical point (CP) on the phase diagram, the mentioned mismatch in energy is vashed out. The phase diagram CP is defined as the doping concentration, where the NSG becomes closed [28, 35-37]. Fermi surface reconstruction

appears here. Behind the CP the mixed carrier system behaves more as a Fermi liquid.

The PG appears as being selective in respect of momentum space regions, where it is created and observed in the corresponding spectral windows. In hole-doped superconductors the PG is merely an "antinodal" ($(\pi, 0)$ -type Brillouin zone centered regions) event. The SCG at underdoping is of $(\pi/2, \pi/2)$ type "nodal" phenomenon. On the route between these points the PG is depressed. The carriers in the regions where the PG is formed must behave as insulating below T*. When passing this curve insulator to metal transitions in the momentum-restricted region are expected and observed [38-40].

2 The pseudogap on multiband background

Cuprates are electronically highly correlated materials. The reconstruction of the crystal interior under doping must be taken into account. The Mott-Hubbard type AF spectrum of a pure sample will be reorganized to form the superconducting playground. This is the second essential result due to doping. The perturbed spectrum includes a qualitatively essential effect. New electron states (bands) inside the charge-transfer gap are created [26,41-46]. One speaks about the creation of midgap-, polaronic-, or defect bands. Doping can regulate the extension of such states and bring them into overlap with the itinerant bands. The superconductivity acquires the multiband nature.

The electron spectrum near the Fermi surface, being actual for the superconductivity, is different for the hole and electron dopings. In the hole case the region near the top of the (mainly) oxygen band between the upper (UHB) and lower Hubbard (LHB) is involved. For electron doping it is the region near the bottom of the UHB.

For superconductivity the part of the electron spectrum near the Fermi surface is acual. The modifications due to doping with the creation of the new (defect) bands appear just here. For hole and electron dopings these spectral regions are different [41, 42, 72]. As largely known, in the hole case it is the area near the top of the (mainly) oxygen band. This band is positioned between the upper (UHB) and lower Hubbard (LHB) bands of the pure AF sample. For the electron doping the region near the bottom of the UHB has been established to be active.

The cuprate superconductivity mechanism remains not well understood at present, c.f. e.g. [47-51, 56]. The approach of our group has been based on a multiband nature of the doped cuprate, with the original idea to use the interband pairing interaction between the itinerant and doping-induced bands. Model realizations of such type approaches for hole-doped cuprates have given general conclusions and results in a qualitative agreement with experimental data [56,57]. The PG on the phase diagram appears here naturally [56-62]. The later consideration of electron-doped systems by analogous interband pairing scheme can be followed in [56,62]. The global similarity of the phase diagrams for both types of doping arise from the "topologically" comparable physical approach. The essential differences between

them stem from the perturbation of different atomic sublattices of the material.

Recently the pairing glue in the cuprates has been identified as being of electronic origin [63]. This justifies the use of interband pairing interaction in our approach (exchange type pair transfer) with its outstadning advantages [64].

In this paper we analyse the PG-s in electron doped cuprates. This problem is not very clear - the recent review paper [65] summarizes that "there are substantial signatures of PG effects in the electron-doped compounds". In this aspect also papers [3, 15, 66-68] can be consulted and theoretical approaches [69-73] must be mentioned.

Our original definition [55, 58, 59] of PG excitations exposes the PG as a natural phenomenon on the multiband background [74]. It is based on the possibility of the appearance of bands intersected or not intersected by the chemical potential (μ). Namely, the PG is considered as the minimal quasiparticle excitation energy of a band (α) not containing μ

$$\Delta_{p\alpha} = \left\{ |\xi_{\alpha} - \mu|_{\min}^2 + \Delta_{\alpha}^2 \right\}^{1/2}. \tag{1}$$

It is supposed that $|\xi_{\alpha} - \mu|_{min} \neq 0$. In (1) ξ_{α} stands for the band energy and Δ_{α} for the SCG gap of the same band. In the case of a nonrigid spectrum μ can be shifted into ξ_{α} , so that $|\xi_{\alpha} - \mu|_{min} = 0$. Then the normal state contribution into $\Delta_{p\alpha}$ vanishes. One reaches a phase diagram CP. Behind a CP the $\Delta_{p\alpha}$ remains represented by the sole SCG Δ_{α} . The reorganizations in the multiband spectrum by doping, or, say, by pressure can influence the PG until its disappearance. The changes in band overlaps become of first significance in the problem of the PG. When the normal state contribution prevails, the PG will be large and repeats practically the behaviour of the NSG. In the neighbourhood of the CP μ enters the given band (or the band reaches μ). The normal state contribution into the PG will be small and both components of $\Delta_{p\alpha}$ can show a comparable magnitude. The quenching of superconductivity (Δ_{α}) can then extract the NSG in this spectral region.

3 Multiband model for an electron-doped cuprate

Basing on versatile knowledge, a 4-band model of the active part of electron-doped cuprate spectrum (Fig. 1) has been proposed [62]. There is the UHB $-(\beta)$ which extends up from its antinodal (AN) $(\pi, 0)$ -type bottom at d_1 . The LHB- (γ) is situated deep and has a nodal (N) $\left(\frac{\pi}{2}, \frac{\pi}{2}\right)$ -type top. Both these bands are of width Δd . Midgap bands appear under the β -band bottom on the account of both Hubbard bands. To differentiate the functionality of the defect states in the momentum space we introduce two subbands. The α_1 one is AN centered with the bottom lying at d. The α_2 one is N-centered with the bottom taken as energy zero. These bands arise from the perturbed copper sublattice and develop with the destruction of the AF order, cf. also the recent calculation [25]. The total number of states (4 bands) is normalized to 1. The concentration of doped electrons for one Cu site per one

spin is c. The undoped material (c=0) has β , γ -weights of states $^{1}/_{2}$. Electron-doping exhausts them to (1/2-c). The α -bands are both of weight c. There is a special spectral weight transfer from the Hubbard components to doping-induced midgap states.

Extended doping shifts the midgap bands towards the β -band bottom and the bare gaps between them become removed. This well-known trend can be taken into account by writing for the top energies of the α_1 - and α_2 -bands $d + \alpha c^2$ and αc^2 correspondingly. This spectral behaviour is decisive for the behaviour of the PG-s on the phase diagram. As a result, the progressive doping leads to the formation of a common carrier family. The constant densities of states read $\rho_{\alpha}(1,2) = (\alpha c)^{-1}$; $\rho_{\beta} = (\frac{1}{2} - c)(\Delta d)^{-1}$, i.e. the midgap bands grow while the Hubbard spectrum tends to total ruination at c = 1/2.

The chemical potential is shifted upward with electron doping starting from a position inside the midgap states as expected, e.g. [65]. One finds the first CP on this route to be reached at $c_0 = (d_1 - d)^{1/2} \alpha^{-1/2}$. Here the first defect-UHB $(\alpha_1 - \beta)$ gap becomes closed. One finds for $c \leq c_0$

$$\mu_1 = d + \alpha c^2,\tag{2}$$

which lies on the higher midgap subband top (α_2 remains filled). It is known [15] that at low dopings the electrons occupy (π , 0)-neighbourhood and extending Fermi surface pockets are formed. For $c \geq c_0$ the upper midgap band and the UHB overlap and define a common ($c \geq c_0$)

$$\mu_2 = (d + \alpha c^2 + d_1 \alpha c \rho_\beta)(1 + \alpha c \rho_\beta)^{-1}.$$
(3)

The second CP (c_x) appears when the nodal midgap states reach the $\alpha_1 - \beta$ mixture. Then the disposition of bands and μ tend to maximize T_c . So, at $c > c_x$ where $c_x = \sqrt{\mu_2(c_x)\alpha^{-1}}$,

$$\mu_3 = (d + 2\alpha c^2 + d_1 \alpha c \rho_\beta)(2 + \alpha c \rho_\beta)^{-1}.$$
 (4)

One really observes that now new spectral intensity around $\left(\frac{\pi}{2}, \frac{\pi}{2}\right)$ emerges to the game [75,78]. This can be attributed to hole-like Fermi surface pockets formation [78]. The joint smooth rising up μ -curve can be found in [62]. Note that the positions of the phase diagram CP-s are essentially determined by the changes in the bands overlap. The same concerns the natural reconstruction of the Fermi surface with doping.

4 Two pseudogaps by electron doping

There are two PG-s in our model connected to the bands β (UHB) and the defect α_2 not intersected by μ at low dopings $c < c_0$. The antinodal UHB PG vanishes as the first CP is

reached. At the same time, the nodal-centered PG has a constant contribution corresponding to the energy difference of both α -bands. One has for $c < c_0$

$$\Delta_{p\beta} = \left[(d_1 - d - \alpha c^2)^2 + \Delta_{\beta}^2 \right]^{1/2},\tag{5}$$

$$\Delta_{p\alpha 2} = \left[d^2 + \Delta_{\alpha}^2 \right]^{1/2}.\tag{6}$$

At c_0 the energy separation of occupied and empty states is removed. This points to the vanishing long-range AF order. The calculation of the magnetic susceptibility in a comparable case has shown [75] that deviations from the half-filling cause rapid reduction of the spin correlation length.

For $c > c_0$ the chemical potential becomes changed to $\mu_2(\text{Eq.3})$ as α_1 - and β -bands overlap. The smaller PG exhibits now an exposed dependence on doping

$$\Delta_{p\alpha^2} = \left[(\mu_2 - \alpha c^2)^2 + \Delta_{\alpha}^2 \right]^{1/2}.$$
 (7)

This gap closes at c_x in the normal state. There remain no NSG near the UHB bottom. One expects that here the tracks of the (short-range) AF correlations, which survived until c_x will be quenched. The AF order vanishes now at all. As a result, two PG-s, having their own relation to the AF order, are expected for electron-doped cuprate superconductors. However, the different assignment of $(\alpha_1; \alpha_2)$ generic momentum space points must be held in mind. The presence of two PG-s in $R_{2-x}Ce_xCuO_4$ seems to follow from the data of [66], see also [65].

The appearance of two PG-s in our model is the result of the supposition that the defect $(\pi, 0)$ and $(\pi/2, \pi/2)$ centered regions of the momentum space are created with a gap between them. Without this assumption there would be only one SCG and one PG present.

5 Results

The mean field Hamiltonian for the proposed 3-band model of the active part includes the UHB and α_1 , α_2 defect bands.

$$H = \sum_{\sigma,\vec{k},s} \epsilon_{\sigma}(\vec{k}) a_{\sigma,\vec{k},s}^{+} a_{\sigma,\vec{k},s} + \Delta_{\beta} \sum_{\vec{k}} [a_{\beta\vec{k}\uparrow} a_{\beta-\vec{k}\downarrow} + a_{\beta-\vec{k}\downarrow}^{+} a_{\beta\vec{k}\uparrow}^{+}]$$
$$- \Delta_{\alpha} \sum_{\vec{k},\alpha} {}^{1,2} [a_{\alpha\vec{k}\uparrow} a_{\alpha-\vec{k}\downarrow} + a_{\alpha-\vec{k}\downarrow}^{+} a_{\alpha\vec{k}\uparrow}^{+}] . \tag{8}$$

Here the band energies $\epsilon_{\sigma} = \xi_{\sigma} - \mu$ are counted from the chemical potential. The LHB remains filled and figures only in the determination of μ . The constant interaction strength (W) of the UHB with both defect bands are taken equal (so $\Delta_{\alpha 1} = \Delta_{\alpha 2}$). The integration (\vec{k}) for defect bands is performed over the corresponding energy intervals with their densities of states.

The Hamiltonian (1) can be simply diagonalized and the results for superconducting gaps with their definition are given by the following expressions ($\Theta = k_B T$)

$$\Delta_{\beta} = 2W \sum_{\vec{k},\alpha}^{1,2} \langle a_{\alpha\vec{k}\uparrow} a_{\alpha-\vec{k}\downarrow} \rangle = W \Delta_{\alpha} \sum_{\vec{k},\alpha}^{1,2} E_{\alpha}^{-1}(\vec{k}) th \frac{E_{\alpha}(\vec{k})}{2\Theta},$$

$$\Delta_{\alpha} = 2W \sum_{\vec{k}} \langle a_{\beta-\vec{k}\downarrow} a_{\beta\vec{k}\uparrow} \rangle = W \Delta_{\beta} \sum_{\vec{k}} E_{\beta}^{-1}(\vec{k}) th \frac{E_{\beta}(\vec{k})}{2\Theta}.$$
(9)

The quasiparticle energies are of an usual form $E_{\sigma} = \sqrt{\epsilon_{\sigma}^2 + \Delta_{\sigma}^2}$. These expressions are used in writing (1) and (9). Gaps (9) tend to zero at a common T_c .

The calculated normal state pseudogaps and the T_c domain for a "representative" electron-doped cuprate are shown in Fig.2. The following input parameters have been used: d = 0.05; $d_1 = 0.15$; $\Delta d = 0.8$ and $\alpha = 11 (\text{eV})$. The interband coupling constant W=0.17 eV between the midgap bands and the upper Hubbard component guarantees then the maximum $T_{cm} = 31 \text{K}$ at c = 0.16. The critical points of the model lie at $c_0 = 0.095$ and $c_x = 0.15$. Reasonable modifications in this parameter set do not lead to essential changes in the general results, cf. [62].

The first larger UHB-associated PG $\Delta_{p\beta}$ falls to zero at c_0 . This point is close to the onset of superconductivity. The calculated [76] plane coherence length starts here a rapid drop, see also [75]. The behaviour of the spin stiffness can be followed in [77]. One expects near c_0 the long-range AF correlations being removed.

The second CP $c_x > c_0$ marks the disappearance of the smaller PG $\Delta_{p\alpha}$ and the vanishing of the survived short-range AF correlations as well, i.e. the AF correlations altogether. This conclusion is to some extent supported by the finding that with approaching the superconducting order (and vanishing PG) the AF correlations are of a short-range and not of the long-range nature [77]. Note also that according to [78] the long-range AF order is not necessary for the development of the PG.

The second CP appears at a position inside the superconducting dome before the maximum T_c is reached at optimal doping. This means that the domains, where (short-range) AF fluctuations are preserved, overlap the superconductivity region markedly. This circumstance is usually mentioned [64], especially in comparison with the hole-doped case. Beyond c_x the low-energy excitation spectrum is expected to be presented by the superconducting gaps Δ_{β}

and Δ_{α} . The large Fermi surface composed of all overlapping bands supports the optimization of T_c .

When analysing the spectral manifestations of multiple pseudo- and superconducting gaps, one must be careful. The smaller gap can remain hidden under the larger one and it can also mask the sharpness of the larger gap. There can be problems with the separation of the constant $\Delta_{p\alpha}$ on the background of $\Delta_{p\beta}$ without considering the angular polarization difference.

The superconducting contribution Δ_{α} into $\Delta_{p\alpha}$ becomes remarkable with an extending doping towards c_x . This is illustrated in Fig.3.

The bands overlap dynamis of the present model allows one to explain some new effects. This can be illustrated by Fig.4, for example, for α_2 and β bands being shifted in the momentum space. Namely, the presence of hole- and electron-type carriers has been detected in electron-doped superconductors [64,76,77]. In the case of the μ position in Fig.4 it intersects both the electron- and hole-like pockets. Analogously, the observation of steep and flat dispersions for carriers [81] can be explained. Also, one can expect the observation of the "foreign"-type carriers as compared with the ones introduced by doping. However, there is an essential requirement that the corresponding "active" PG has been closed (upper band in Fig.4).

In addition, paper [82] states that although both hole and electron pockets are known in electron-doped cuprate superconductors, there ,,is no evidence so far of electron pockets in hole-doped cuprates. This finding can be explained by using the mentioned relative behaviour of the PG and the ,,foreign carriers effect. For electron-doped materials it is known, as also found in the present work, that the PG (curve 3 in fig.2) touches the T_c domain at a relatively ,,early level. Contrary to the hole-doped materials, the end of the PG is found (also calculated [56]) to extend nearly until the overdoped end of the T_c domain. The doping interval for the effect under consideration will be narrow. In general, the observation of foreign carriers as compared to the ones introduced by doping is expected to start with the vanishing of the corresponding PG.

An extended comparison of the present model, formulated for a "typical" electron-doped cuprate superconductor, with the experimental data is a complicated task. The mainly investigated systems are of the type $R_{2-x}M_xCuO_4$ (R – rare earth; M – Ce or Th). The data for a distinct material and (naturally) between various systems are dispersive. It seems that the general results obtained by our model mechanism justify its use in various analyses. Especially the rised problem of the existence of two PG-s in electron-doped cuprates is of interest. The theoretical approach itself can be improved in various aspects, e.g. taking the pairing strengths for the $\beta - \alpha 1$ and $\beta - \alpha 2$ channels to be different, or precising the parameter set.

6 Conclusion

In conclusion, the present model approach suggests the appearance of two pseudogaps in electron-doped cuprates. These gaps are connected with the destruction of long- and short-range antiferromagnetic correlations. There are two critical points on the doping phase diagram. The larger one is centered in the antinodal momentum space region at small dopings. The second one is expected to be mainly a near-nodal event. Its doping dependence is exposed behind the first critical point. The second critical point lies before the maximal T_c . Antiferromagnetic and superconducting domains overlap markedly.

Nowadays multiband pairing schemes are applied to novel, famous or artificial superconducting systems. The appearance of a PG-type excitation in the spectra of these materials can be considered, as illustrated also in the present work, to be an indication of a multi-component (probably three-band [61]) nature of the superconducting playground. On the other hand, in the case of a multicomponent Fermi surface intersected simultaneously by the chemical potential, one can expect high transition temperatures by the functioning of interband coupling channels (missing PG).

This work was supported by the European Union Regional Development Fund (Centre of Excellence ,,Mesosystems: Theory and Applications", TK114) and the Estonian Science Foundation grant No 8991.

References

- [1] T. Timusk and B. Statt, Rep. Prog. Phys. 62 (1991) 61.
- [2] T. Timusk, Solid State Commun. 127 (2003) 337.
- [3] A. Damascelli, Z. Hussain and Z.-X. Shen, Rev. Mod. Phys. 75 (2003) 473.
- [4] D. N. Basov and T. Timusk, Rev. Mod. Phys. 77, (2005) 721.
- [5] P. A. Lee, N. Nagaosa and X. G. Wen, Rev. Mod. Phys. 78 (2006) 18.
- [6] J. L Tallon et al., Physica C 415 (2004) 9.
- [7] S. Hüfner et al., Pep. Prog. Phys. 71 (2008) 062501.
- [8] R. Daou et al., Nature 463 (2010) 519.
- [9] T. M. Rice, K.-Y. Yang and F. C. Zhang, Rep. Prog. Phys. 75 (2012) 016502.
- [10] T. Yoshida et al., J. Phys. Soc. Jpn. 81 (2012) 011006.
- [11] S. H. Naqib et al., Phys. Rev. B 71 (2005) 054502.

- [12] L. P. Gor'kov and G. B. Teitel'baum, Phys. Rev. Lett. 97 (2006) 247003.
- [13] L. Yu et al., Phys. Rev. Lett. 100 (2008) 177004.
- [14] T. Kondo et al., Nature Phys. 7 (2011) 21.
- [15] K. Okada, J. Phys. Soc. Jpn. 78 (2009) 034725.
- [16] N. Bergeal et al., Nature Phys. 4 (2008) 608.
- [17] R. Khasanov et al., Phys. Rev. Lett. 101 (2008) 227002.
- [18] J.-H. Ma, et al., Phys. Rev. Lett. 101 (2008) 207002.
- [19] A. Pushp, et al., Science 324 (2009) 1689.
- [20] A. Bianconi et al., Solid. State. Commun. 102 (1997) 369.
- [21] A. M. Gabovich et al., Adv. Cond. Mat. Phys. 2010 (2010) 68170.
- [22] F. Laliberté et al., Nature Commun. 2 (2011) 432.
- [23] C. V. Parker et al., Nature 468 (2010) 677.
- [24] C. M. Varma and L. Zhu, Phys. Rev. Lett. 98 (2007) 177004.
- [25] V. Seagnoli et al., Science 332 (2011) 696.
- [26] M. J. Lawler et al., Nature 466 (2010) 347.
- [27] M. Hashimoto et al., Nature Phys. 6 (2010) 414.
- [28] J. L. Tallon and J. N. Loram, Physica C 349 (2001) 53.
- [29] J. Tahir-Kheli and W. A. Goddard, Phys. Chem. Lett. 2 (2011) 2326.
- [30] S. K. Nair et al., Phys. Rev. B 82 (2010) 212503.
- [31] V. D. Lakhno and E. L. Nagaev, Fiz. Tverd. Tela. 18 (1976) 3429.
- [32] V. Hizhnyakov, N. Kristoffel and E. Sigmund, Physica C 160 (1989) 435.
- [33] R. K. Kremer et al., Zs. f. Physik B 86 (1992) 319.
- [34] Y. Kohsaka et al., Nature Phys. 8 (2012) 534.
- [35] C. Varma, Nature 468 (2010) 184.
- [36] L. Taillefer, Annu. Rev. Condens. Matter Phys. 1 (2010) 51.

- [37] D. Di Castro et al., Eur. Phys. J. B 18 (2000) 617.
- [38] P. Calvani, Phys. Stat. Solidi b 237 (2003) 194.
- [39] F. Venturini et al., Phys. Rev. Lett. 89 (2002) 107003.
- [40] P. Fournier et al., Phys. Rev. Lett. 81 (1998) 4720.
- [41] T. Takahashi et al., Physica C 170 (1990) 416.
- [42] C. Uchida et al., Phys. Rev. B 43 (1991) 7942.
- [43] M. B. J. Meinders, H. Eskes and G. A. Sawatzky, Phys. Rev. B 48 (1993) 3916.
- [44] P. Schwaller et al., Eur. Phys. J. B 18 (2000) 215.
- [45] A. Bianconi et al., Physica C 296 (1998) 269.
- [46] A. Ino et al., Phys. Rev. B 65 (2002) 094504.
- [47] A. S. Alexandrov, J. Supercond. 18 (2005) 3.
- [48] R. Micnas, S. Robaszkiewicz and A. Bussmann-Holder, Physica C 387 (2003) 58.
- [49] H. Keller and A. Busmann-Holder, Adv. in Cond. Matter Phys. ID393526 (2010).
- [50] D. Innocenti et al., Phys. Rev. B 82 (2010) 184528.
- [51] H. Kamimura et al., Theory of Copper Oxide Superconductors, Springer, Berlin, 2005.
- [52] P. Konsin, N. Kristoffel and T. Ord, Phys. Lett. A 129 (1988) 339.
- [53] N. Kristoffel, P. Konsin and T. Örd, Rivista Nuovo Cim. 17 (1994) 1.
- [54] N. Kristoffel, Phys. Stat. Solidi b 210 (1998) 195.
- [55] N. Kristoffel and P. Rubin, Physica C 356 (2001) 171.
- [56] N. Kristoffel, P. Rubin and T. Örd, Intern. J Modern Phys. B 22 (2008) 5299.
- [57] N. Kristoffel, P. Rubin and T. Ord, J. Phys. Conf. Ser. 108 (2008) 012034.
- [58] N. Kristoffel and P. Rubin, Solid State Commun. 122 (2002) 265.
- [59] N. Kristoffel and P. Rubin, Physica C 402 (2004) 257.
- [60] N. Kristoffel and P. Rubin, Phys. Lett. A 374 (2009) 70.
- [61] N. Kristoffel and P. Rubin, Intern. J Modern Phys. B 26 (2012) 1250144.

- [62] N. Kristoffel and P. Rubin, Phys. Lett. A 372 (2008) 930.
- [63] V. M. Krasnov, S.-O. Katterwe and A. Rydh, Nature Commun. 4 (2013) 3970.
- [64] N. Kristoffel: in Progress in Superconductivity Research, Ed. O. A. Chang, Npva Sci. Publ., NY, 2008, p.7.
- [65] N. P. Armitage, P. Fournier and R. L. Greene, Rev. Mod. Phys. 82 (2010) 2421.
- [66] L. Alff et al., Nature (Lett.) 422 (2003) 698.
- [67] K. Jin et al., Nature (Lett.) 476 (2011) 73.
- [68] S. Basak et al., Phys. Rev. B 85 (2012) 075104.
- [69] Y. Onose et al., Phys. Rev. Lett. 87 (2001) 217001.
- [70] C. Kusko et al., Phys. Rev. B 66 (2002) 140513(R).
- [71] B. Kyung et al., Phys. Rev. Lett. 93 (2004) 147004.
- [72] M. Taguchi et al., Phys. Rev. Lett. 95 (2005) 177002.
- [73] C. Weber, K. Haule and G. Kotliar, Nature Phys. 6 (2010) 574.
- [74] N. Kristoffel, in: J. E. Nolan (Ed.), Superconductivity Research Advances, Nova Sci. Publ. Inc., 2007, p.225.
- [75] A. Sherman and M. Schreiber, Phys. Rev. B 76 (2007) 235112.
- [76] N. Kristoffel and P. Rubin, in: Electron Transport in Nanosystems, Ed. J. Bonča, S. Kruchinin, Springer Sci, Dordrech, 2008, p. 179.
- [77] M. Motoyama et al., Nature 445 (2007) 186.
- [78] B. Kyung et al. Phys. Rev. Lett., 93, (2004) 147004.
- [79] H. Matsui et al., Phys. Rev. Lett. 94 (2005) 047005.
- [80] Y. Dagan and R. L. Greene, Phys. Rev. B 76 (2007) 24506.
- [81] S. Park et al., Phys. Rev. B 75 (2007) 060501(R).
- [82] S. Chakravarty, Rep. Prog. Phys. 74 (2011) 022501.

Figure captions

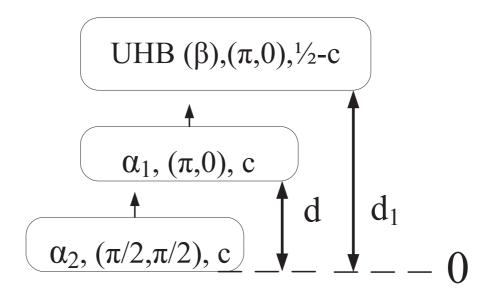
Figure 1. The bands scheme with doping-created midgap (defect) bands (α_1, α_2) between

the LHB and UHB. O denotes the mainly oxygen band. Nodal symbols belong to band tops.

Figure 2. The doping phase diagram of an electron-doped cuprate superconductor with the T_c dome and the larger (1) and smaller (2) normal state PG-s.

Figure 3. The behaviour of the PG $\Delta_{p_{\alpha}}$ (1) near the second critical point c_x . Behind c_x it continues as Δ_{α} . For $c < c_x$ the Δ_{α} (2) is hidden in $\Delta_{p\alpha 2}$. (3)- the normal state contribution to the PG.

Figure 4. Bands crossing at different momentum points produce electron and hole-pockets at the given μ .



O

LHB $(\gamma),(\pi/2,\pi/2),\frac{1}{2}-c$

